

## Article

# Impact of Zinc Oxide Nano Particles, Poly Vinyl Alcohol, and Natural Polymers on Quality Characteristics of Nanocomposite Film

Gurpreet Singh <sup>1</sup>, Sivakumar Shanmugam <sup>1,\*</sup>, Rekha Chawla <sup>1</sup> , Nitika Goel <sup>1</sup>, Gopika Talwar <sup>1</sup>, Santosh Kumar Mishra <sup>1</sup>  and Manish Kumar Chatli <sup>2</sup>

<sup>1</sup> College of Dairy Science and Technology, Guru Angad Dev Veterinary & Animal Sciences University (GADVASU), Ludhiana 141004, India

<sup>2</sup> Department of Livestock Products Technology, College of Veterinary Science, Guru Angad Dev Veterinary & Animal Sciences University (GADVASU), Ludhiana 141004, India

\* Correspondence: sivakumarshanmugam60@gmail.com

**Abstract:** The use of biodegradable films to replace the synthetic polymers prepared from natural polymers has been strongly limited owing to their poor barrier and mechanical properties. The modification was carried out with a partial replacement of natural polymers with synthetic polymer, such as PVA (poly vinyl alcohol), to increase the barrier properties of the film. The addition of an active ingredient in the form of nanoparticles such as Zinc Oxide (ZnO), enhanced the properties of the packaging materials compared to the conventional composite film, to which sonication imparted an excellent dispersion of nanoparticles in the slurry. The film thickness, water vapor permeability, film solubility, and mechanical properties of the composite, the composite with PVA, and the composite with PVA and ZnO nanoparticle film (active film) values differed significantly ( $p < 0.05$ ) between the samples. The Z-average diameters of the composite slurry, the composite with PVA slurry, and the composite with PVA and ZnO nanoparticle slurry ranged from 242.20 to 1021.03 in nanometers (d-nm). The PDI and zeta potential of the samples were also analyzed. The antibacterial activity of the nanoparticles showed a distinct inhibition against Gram-positive *Bacillus cereus* and Gram-negative *Escherichia coli* in the treated films counterpart to the control films. The active film conferred excellent mechanical and barrier properties, including antibacterial properties.

**Keywords:** natural polymers; synthetic polymers; ZnO nanoparticles; PVA; quality characteristics; nanocomposite film



**Citation:** Singh, G.; Shanmugam, S.; Chawla, R.; Goel, N.; Talwar, G.; Mishra, S.K.; Chatli, M.K. Impact of Zinc Oxide Nano Particles, Poly Vinyl Alcohol, and Natural Polymers on Quality Characteristics of Nanocomposite Film. *Coatings* **2023**, *13*, 420. <https://doi.org/10.3390/coatings13020420>

Academic Editor: Philipp Vladimirovich Kiryukhantsev-Korneev

Received: 28 December 2022

Revised: 29 January 2023

Accepted: 1 February 2023

Published: 13 February 2023



**Copyright:** © 2023 by the authors. Licensee MDPI, Basel, Switzerland. This article is an open access article distributed under the terms and conditions of the Creative Commons Attribution (CC BY) license (<https://creativecommons.org/licenses/by/4.0/>).

## 1. Introduction

Packaging is an important aspect of preserving the quality and safety of various food products, along with their shelf-life extension. The development of biopolymer-based packaging materials to replace synthetic polymers has become a growing field of interest due to serious environmental concerns. Several biopolymers have been exploited to develop eco-friendly food packaging materials, viz. polysaccharides, proteins, and lipids [1]. Researchers such as De Azeredo [2] observed that the production of composite films using different fillers is a better way of improving the performance of biodegradable films. In addition, the combination of polymers, i.e., composite polymers, provides various added advantages compared to single polymers. Currently, composites typically consist of a polymer matrix or continuous phase, and a filler or discontinuous phase. In this regard, Whey protein concentrate (WPC) and Whey protein isolate (WPI) are biopolymers that have received much attention for use as a potential edible or biodegradable food packaging material owing to their production of transparent films and coatings that can act as an excellent oxygen barrier property at very low levels of RH [3,4]. Additionally, other plant-based biopolymers, such as starch and carrageenan, have been evaluated for their film-forming applications in food packaging areas [5,6]. However, the use of biodegradable

films prepared from natural polymers has been strongly limited due to their poor barrier and mechanical properties.

Therefore, many studies have recommended the modification of natural polymeric film employing partial replacement of natural polymers with synthetic polymers, such as poly vinyl alcohol (PVA), to increase their barrier and mechanical properties. It is a synthetic water-soluble polymer with excellent film-forming, emulsifying, and adhesive properties [7], and imparts good tensile strength (TS) and biodegradability, and hence has been used in many biomaterial applications. PVA has been approved for use in packaging meat and poultry products by the USDA [8]. Additionally, in the film-making process, glycerol has shown itself to be a favorable plasticizer in composite films because of its plasticization ability due to its low molecular weight [9].

A low level of nanoparticles, such as zinc oxide (ZnO), is sufficient to change the properties of packaging materials without significant changes in their density, transparency, and processing characteristics [10]. They have been widely used in daily life, e.g., in medical devices, drug delivery, and cosmetics [11]. Similarly, these nanoparticles exhibit antibacterial properties in both microscale and nanoscale formulations [12]. These results also indicate that films with nanoparticles can be considered a safe packaging material. In addition, film preparational methodology, employing high-power ultrasonication, has been known to create better dispersions of nanoparticles during mixing [13]. Keeping in mind the above-mentioned points, the present study was carried out to incorporate zinc oxide nanoparticles and PVA with the quality characteristics of nanocomposite film.

## 2. Materials and Methods

### 2.1. Chemicals Required for Film Formation

Corn starch (maize) and carrageenan were procured from the Central Drug House, Pvt. Ltd., Delhi, India. Whey protein concentrate (WPC) and whey protein isolate (WPI) were procured from Mahaan Proteins Ltd., Kosi Kalan (U.P), India. Poly vinyl alcohol (PVA) and zinc oxide (ZnO) nanoparticles were procured from Sigma Aldrich Chemicals Pvt. Ltd., Delhi, India, whereas glycerol was procured from Loba Chemical Pvt. Ltd., Mumbai, India.

### 2.2. Preparation of Corn Starch/WPI/WPC/Carrageenan Composite Film

The composite film consisted of corn starch (maize), WPI, WPC, and carrageenan prepared using the casting method. Initially, WPC (2.5%) and WPI (2.5%) were added to distilled water, and for complete dissolution, a magnetic stirrer was utilized. To this mixture, carrageenan (0.25%) and corn starch (maize) (2.5%) were added with continuous stirring, leading to the gelatinization of corn starch (maize) at 60–70 °C; glycerol (2%) was then added and mixed properly with the help of a magnetic stirrer. Plastic Petri dishes (150 mm) were used for the formation of film using the film-casting method. After the homogenization process, the slurry was kept undisturbed for 30–45 min for the settlement of bubbles and to decrease the temperature of the film-forming solution. The dishes were then transferred to a hot air oven (MAC) at 40 °C for 16–17 h for proper and complete drying. As a precautionary measure, to suppress the growth of fungi and unwanted bacteria, a fumigation of the hot air oven was undertaken before the experimentation.

### 2.3. Preparation of Corn Starch/WPI/WPC/Carrageenan Composite Film with PVA

PVA (0.5%) was added to water for proper mixing on a hot plate magnetic stirrer. After the proper mixing of the PVA, whey protein concentrate, whey protein isolate, and carrageenan were added. After the proper mixing stage, the corn starch (maize) was added to the slurry, and the rest of the procedure, as described above for the composite film [14], was followed.

### 2.4. Preparation of Corn Starch/WPI/WPC/Carrageenan/PVA/ZnO nanocomposite Film

The above-mentioned procedures were followed, up to the gelatinization of the corn starch (maize), after which ZnO nanoparticles (finalized after preliminary trials amongst

(AgO, TiO<sub>2</sub>, and ZnO) (0.3%) with glycerol) were added to the slurry, and their initial mixing was completed by a magnetic stirrer (Singh [15]). Thus, sonication was achieved with the help of an ultrasonicator (40 Amp, for 10 min) for the proper mixing of nanoparticles as per the procedure demonstrated by Sivakumar et al. [16,17]. After the gelatinization and sonication processes, the casting was carried out in polypropylene Petri dishes for the film formation. The temperature–time combination used for the formation and drying of the film was 40 °C for 16–17 h (Figure 1a,b).

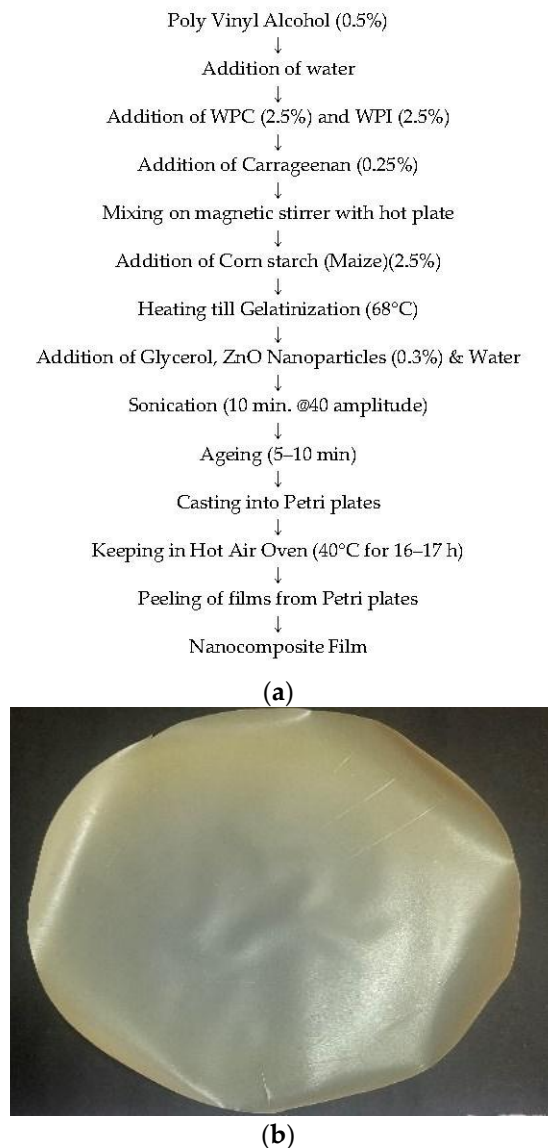


**Figure 1.** (a): Flow diagram for preparation of optimized nanocomposite film; (b): Corn starch (Maize) + WPC & WPI + PVA + carrageenan + glycerol + ZnO (active film).

### 2.5. Characterization of Slurry Used for Film Formation

The viscosity of the slurry was checked with the Brookfield Viscometer employing spindle—LV-01. The speed of the spindle was kept at 20 RPM for 3 min with 30 s shearing. A digital pH meter (Mettler Toledo, Columbus, OH, USA) was used to measure the pH during the investigation. The particle size analyzer average (d-nm), the zeta potential, and the poly dispersibility index (PDI) were measured by a dynamic light scattering (DLS) device (Zetasizer Nano-ZS, Malvern Instruments Ltd., Worcestershire, UK), as per the manufacturer's instructions.

## 2.6. Characterization of Film

Six measurements were taken at different points randomly selected from each film to avoid an error, and an average was taken using a digital micrometer. The water solubility of the film was measured using the procedure followed by Singh et al. [18].

The water vapor permeability (WVP) was measured using a modified method given by [19]. The film was sealed on a modified test cell (beaker) with 30 mL of distilled water, and then kept in a desiccator containing a pre-dehydrated silica gel. Silica gels were dried at 180 °C/3 h for these measurements. The whole assembly was kept at 25 °C for 24 h, and the loss of weight was measured. The WVP was estimated as indicated in the equation:

$$\text{WVP} = \Delta W / (\Delta t \times A)$$

Here,  $\Delta W$  is the weight loss of the test cell.

$\Delta t$  is the time of storage.

$A$  is the area of exposed film.

A UV-VIS spectrophotometer (Systronics double-beam spectrophotometer 2203 smart) was used to find out the light transmittance (%) of the film at the wavelength of 660 nm. A water activity meter (Aqua lab series, 4TE) was used to measure the water activity of the film. The biodegradation of the film was measured using the procedure followed by Al-Sahlany [20]. A CR-400 Konica chroma meter (Konica Minolta, Japan) was used to find out the instrumental color value of  $L^*$ ,  $a^*$ , and  $b^*$  of the films as per the manufacturer instructions. The antimicrobial activity of the slurry and the film was tested against the food spoilage pathogens using the agar spot test by Shokryazdan et al. [21].

## 2.7. Mechanical Properties of Film

The tearing strength and the puncturing strength were as measured by the TMS-Pro Food Technology Corporation texture analyzer. The minimum force required to rupture and pierce the film was calculated in N (Newton). For the estimation of the tearing strength, the film was placed (7 cm × 2 cm) between two grips or clumps. The distance between the two grips was 5 cm, and the speed of the instrument was 1 mm/s. With respect to the estimation of the puncturing strength, the films were measured by placing a round film strip (with a diameter of 6–7 cm) on a circular holder. The speed of the instrument was 1 mm/s. A 5 mm diameter probe was used for piercing the film sample.

### 2.7.1. Scanning Electron Microscopy (SEM)

The microstructure of the film samples on the film surface was observed using a scanning electron microscope (JEOL JSM-6510, Tokyo, Japan) at an accelerating voltage of 15 kV. The film piece was placed on a stub using a two-sided carbon tape, and then sputter-coated with a thin layer of gold prior to analysis. The sampling procedure was carried out at an ambient temperature. The image was taken with the help of instrument software with an initial grip distance of 100 mm and a crosshead speed of 50 mm/min during analysis.

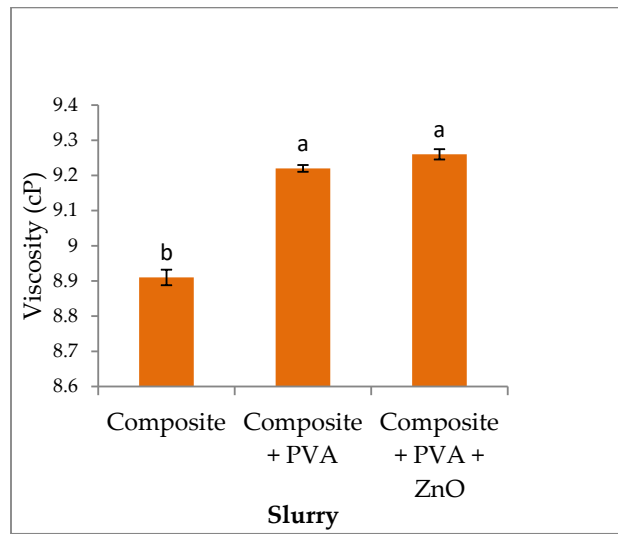
### 2.7.2. Statistical Analysis

The data obtained during the present investigation were analyzed by employing SPSS 25.0 statistical software. The quality parameters of the slurry and film were assessed by employing a one-way analysis of the variance (ANOVA) with six replications at a 5 per cent level of significance ( $p < 0.05$ ).

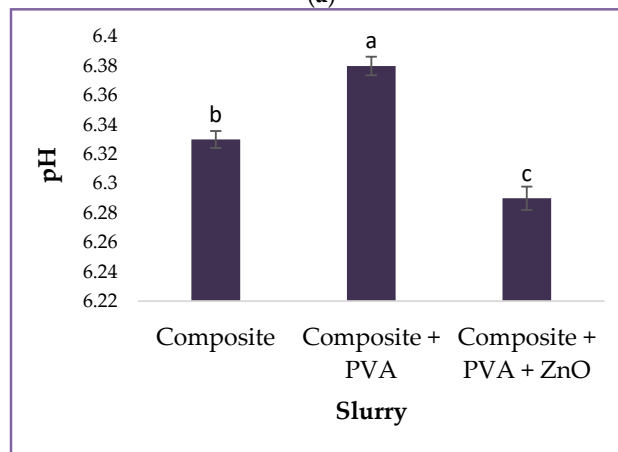
## 3. Results and Discussions

### 3.1. Properties of Different Type of Slurries

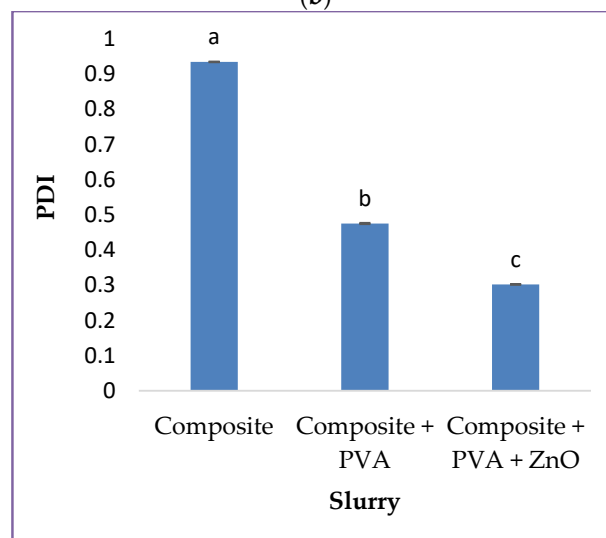
The properties of the different types of slurries are presented in Figure 2.



(a)



(b)



(c)

Figure 2. Cont.

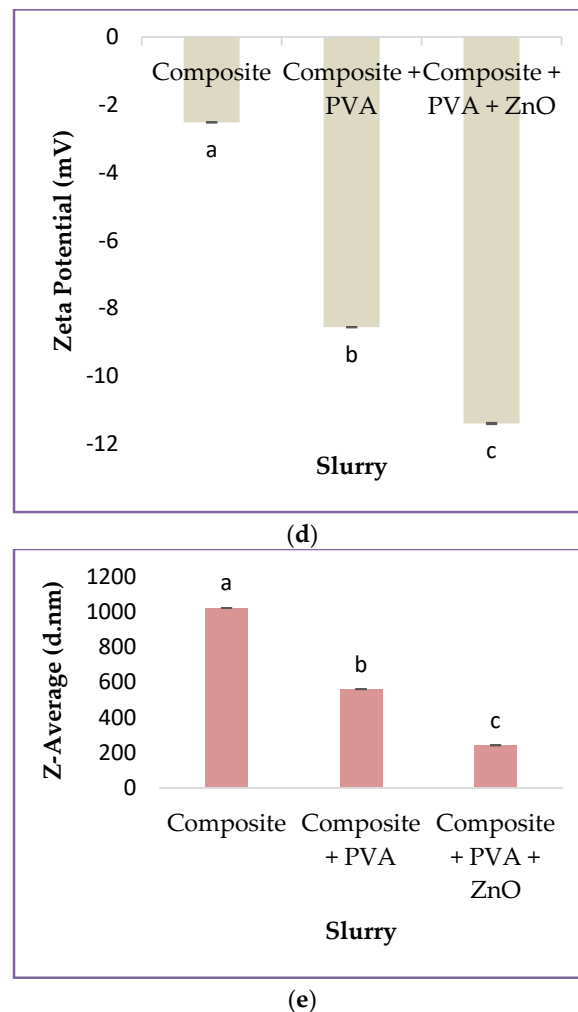


**Figure 2.** (a–e) Properties of different types of slurries used for film formation: (a) viscosity, (b) pH, (c) PDI, (d) zeta potential, and (e) Z-average. Means with different superscripts <sup>a–c</sup> differ significantly ( $p < 0.05$ ).

#### Viscosity

The viscosity of the composite slurry, the composite with PVA slurry, and the composite with PVA and ZnO nanoparticle slurry ranged from 8.91 to 9.26 cP, as shown in Figure 2a. There was a non-significant difference ( $p < 0.05$ ) with the addition of the ZnO nanoparticle-incorporated nanocomposite slurry and the slurry of the composite with the PVA. The results were correlated with Gurpreet and Singh [22], who stated that the addition of nanoparticles had no significant effect on the viscosity of the slurries.

#### pH

The pHs of the composite slurry, the composite with PVA slurry, and the composite with PVA and ZnO nanoparticle slurry were 6.33, 6.38, and 6.29, respectively. The pH values differed significantly ( $p < 0.05$ ) between the samples (Figure 2b). The slurry pH plays a critical role in the formation of the films and their morphologies [23]. Films prepared with acidic pH improved the water vapor permeability, transparency, solubility, and thermal stability as compared to the alkaline pH.

#### Polydispersity Index (PDI)

The PDIs of the composite slurry, the composite with PVA slurry, and the composite with PVA and ZnO nanoparticle slurry ranged from 0.302 to 0.934, as shown in Figure 2c. The PDI values differed significantly ( $p < 0.05$ ) between all the samples. The results correlated with those of Gurpreet and Singh [22], who suggested that the nanoemulsion PDI values between (0 and 1) might be correlated with more stability.

### Zeta Potential

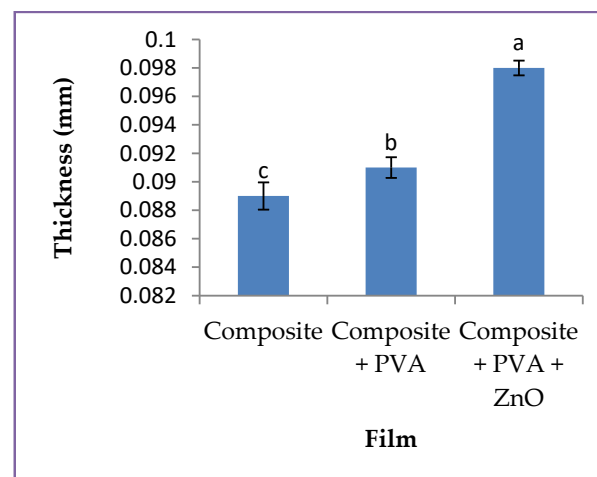
The zeta potential of the composite, the composite with PVA, and the composite with PVA and ZnO nanoparticle slurry is shown in Figure 2d. The zeta potential of the composite slurry, the composite with PVA slurry, and the composite with PVA and ZnO nanoparticle slurry ranges from  $-2.52$  mV to  $-11.40$  mV. Sonication has been proven to be a good method for the dispersion of nanoparticles in the slurry. There was a significant difference ( $p < 0.05$ ) between all the samples. Similar findings were reported by Qi et al. [24] and Marsalek [25], who found that the zeta potential is a measure of the magnitude of the electrostatic or the charge repulsion/attraction between particles. Furthermore, this is one of the fundamental parameters known to affect stability. In addition, a lower value shows a higher van der Waal attraction, which causes aggregation and thus instability [26].

### Z-Average

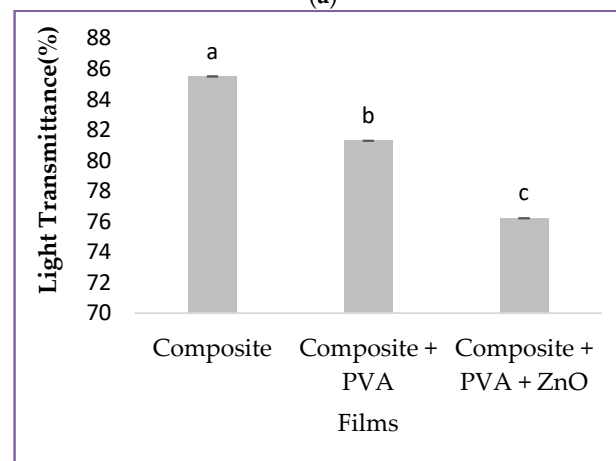
The Z-average of the composite slurry, the composite with PVA slurry, and the composite with PVA and ZnO nanoparticle slurry ranged from 1021.03 to 242.20 d-nm, as shown in Figure 2e. There were significant differences ( $p < 0.05$ ) between all the samples. Similar results were reported by Qi et al. [24] and Marsalek [25]. The z-average value is an intensity-weighted mean diameter of the bulk population of the sample.

### 3.2. Properties of Different Type of Films

The properties of different types of films, such as the film thickness, light transmittance, water activity, water vapor permeability (WVP), film solubility, tensile strength, and puncturing strength are shown in Figure 3.

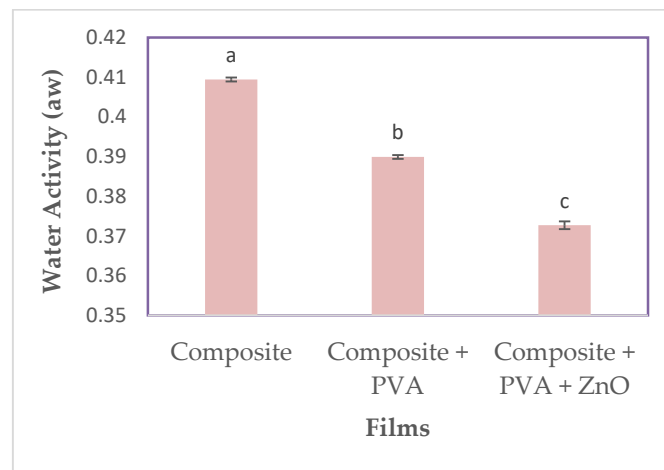


(a)

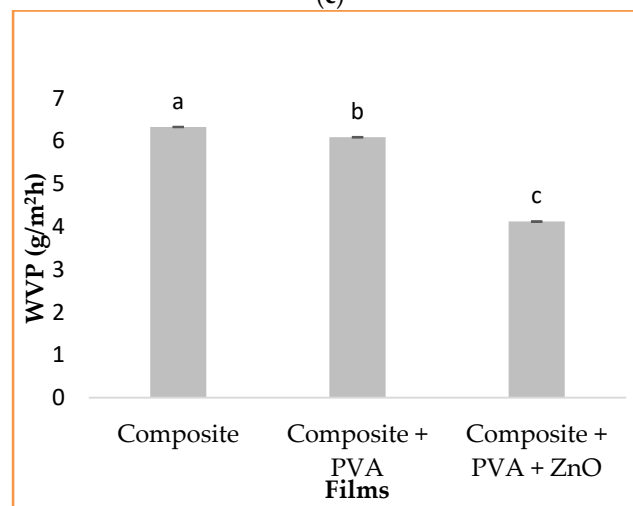


(b)

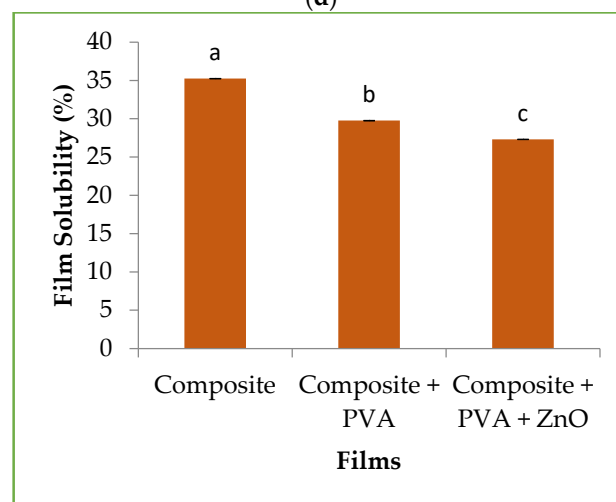
Figure 3. Cont.



(c)



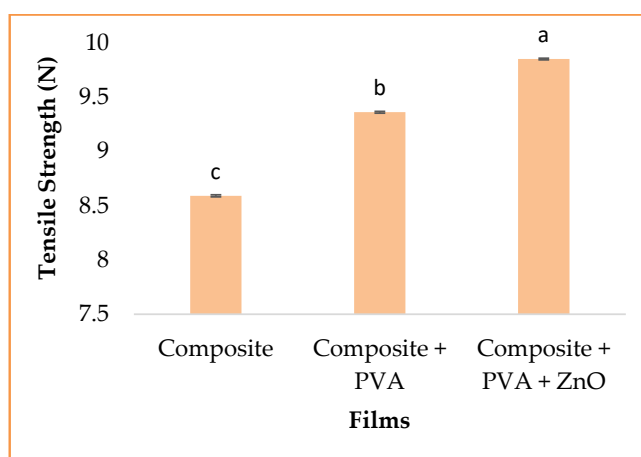
(d)



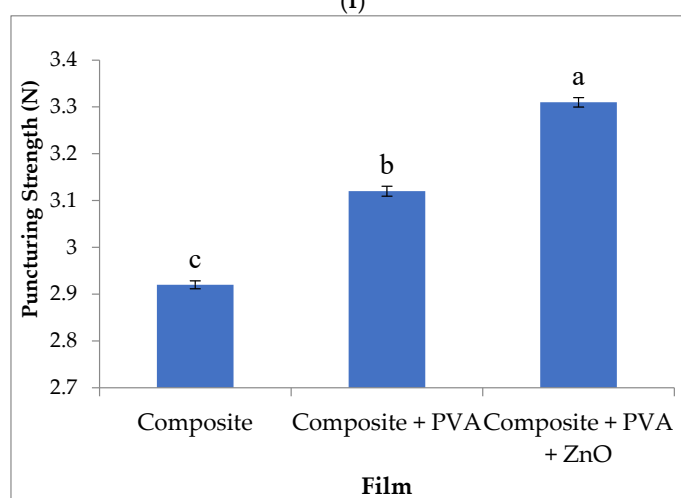
(e)

Figure 3. Cont.





(f)



(g)

**Figure 3.** (a–g) Properties of different types of films. Means with different superscripts <sup>a–c</sup> differ significantly ( $p < 0.05$ ).

#### Film thickness

The film thickness of the composite, the composite with PVA, and the composite with PVA and ZnO nanoparticle film is shown in Figure 3a. The film thickness of the composite, the composite with PVA, and the composite with PVA and ZnO nanoparticles ranged from 0.089 to 0.098 mm. The results show that the addition of PVA and ZnO nanoparticles increased the thickness compared to the composite film alone. Similar findings were reported by Gharoy Ahangar et al. [27], Rhim et al. [28], and Ngo et al. [29]. The values differed significantly ( $p < 0.05$ ) between the samples mentioned above.

#### Light transmittance

The light transmittance of the composite film, the composite with PVA film, and the composite with PVA and ZnO nanoparticle film ranged from 76.21 to 85.51 per cent. The light transmittance of the composite film, the composite with PVA film, and the composite with PVA and ZnO nanoparticle film is shown in Figure 3b. Due to the addition of PVA and ZnO to the films, the thickness increased, which resulted in a decrease in light transmittance. The light transmittance values differed significantly ( $p < 0.05$ ) for all the samples. Similar results were observed by the Yang et al. [30] and Atta et al. [31].

#### Water Activity

The water activity of the composite film, the composite with PVA film, and the composite with PVA and ZnO nanoparticle film ranged from 0.3727  $a_w$  to 0.4094  $a_w$ , as shown in Figure 3c. There were significant differences ( $p < 0.05$ ) between all the samples.

#### Water Vapor Permeability (WVP)

The water vapor permeability of the composite, the composite with PVA, and the composite with PVA and ZnO nanoparticle film ranged from 4.12 to 6.33 g/m<sup>2</sup>h, as shown in Figure 3d. It could be speculated that nanoparticles made the film more hydrophobic and filled the pores in the macromolecules structures, which decreased the permeability of the water vapors and added nanoparticles to the sites on the composite films that normally would be occupied by water. The results correlated with the findings of Ngo et al. [29], Gharoy Ahangar et al. [27], Nafchi et al. [32], and Saputri et al. [33] who stated that the permeability of the films was due to the moisture transfer between food and the atmosphere, which ultimately determines the deteriorative changes in dairy products. The WVP values differed significantly ( $p < 0.05$ ) between all the samples.

#### Film solubility

The film solubility of the composite film, the composite with PVA film, and the composite with PVA and ZnO nanoparticle film is shown in Figure 3e. The film solubility value is an important functional property for the film based on biopolymers, which is related to the hydrophilicity of the materials. The film solubility of the composite film, the composite with PVA film, and the composite with PVA and ZnO nanoparticle film ranged from 35.25 to 27.31%. The film solubility values differed significantly ( $p < 0.05$ ) between the samples of the control and the experimental. The results are correlated with the findings of Nafchi et al. [32], Ngo et al. [29], and Rhim et al. [28].

#### Tensile strength

The tensile strength of the composite film, the composite with PVA film, and the composite with PVA and ZnO nanoparticle film ranged from 8.59 to 9.85 N, as shown in Figure 3f. The tensile strength increased with the addition of ZnO nanoparticles to the active films. The incorporation of nanoparticles into the film solutions effectively enhanced the interfacial interactions within the control film network via the establishment of hydrogen and covalent bonds between nanoparticles and other polymer molecules. The values differed significantly ( $p < 0.05$ ) between all the samples. The results were previously reported by Akhavan et al. [34], Vasile et al. [11], Ahmad et al. [35], and Wu et al. [36].

#### Puncturing strength

The puncturing strength of the composite film, the composite with PVA film, and the composite with PVA and ZnO nanoparticle film is shown in Figure 3g. The puncturing strength of the composite film, the composite with PVA film, and the composite with PVA and ZnO nanoparticle film ranged from 2.92 to 3.31. The values differed significantly ( $p < 0.05$ ) between the samples. The same results were previously reported by Vasile et al. [11], Ahmad et al. [35], and Wu et al. [36].

### 3.3. Colour

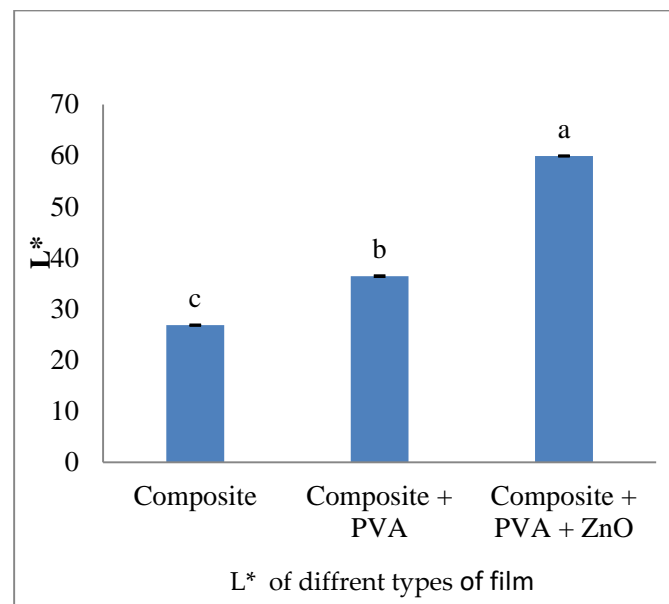
The color properties ( $L^*$ ,  $a^*$ , and  $b^*$ ) of the different types of films are shown in Figure 4.

#### ( $L^*$ )

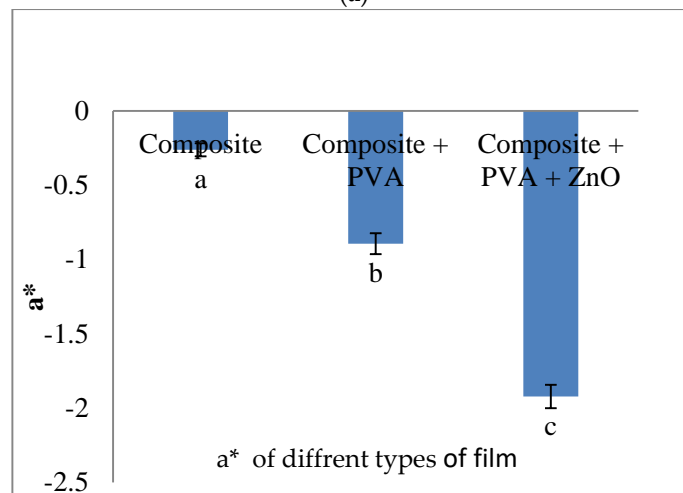
The  $L^*$  of the composite film, the composite with PVA film, and the composite with PVA and nanoparticle film ranged from 26.83 to 59.93, as shown in Figure 4a. The  $L^*$ (lightness) value of the ZnO nanocomposite film was significantly higher than that of other films. The  $L^*$  (lightness) value of the composite with PVA film was lower than the ZnO nanocomposite films, but higher than composite film. These were significant differences ( $p < 0.05$ ) between the samples.

#### ( $a^*$ )

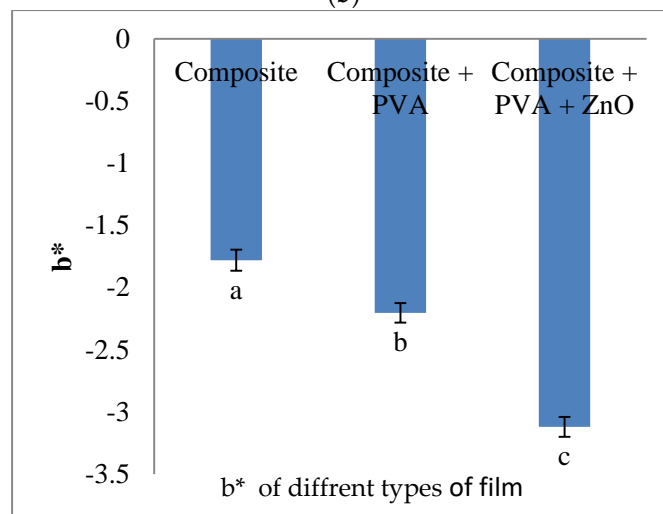
The  $a^*$  of the composite film, the composite with PVA film, and the composite with PVA and ZnO nanoparticle film ranged from  $-0.26$  to  $-1.92$ , as shown in Figure 4b. There was a non-significant difference in the  $a^*$  value between samples. These results indicate that the lightness of the film samples increased with the decrease in greenness. There were significant differences ( $p < 0.05$ ) between the samples.



(a)



(b)



(c)

**Figure 4.** (a–c) Color profiling of different types of films. Means with different superscripts <sup>a–c</sup> differs significantly ( $p < 0.05$ ).

(b\*)

The  $b^*$  of the composite film, the composite with PVA film, and the composite with PVA and ZnO nanoparticle film ranged from  $-3.12$  to  $-1.78$ , as shown in Figure 4c. There were significant differences ( $p < 0.05$ ) between the samples.

The results obtained for color values correlated with the findings of Kumar et al. [37], Amjadi et al. [38], and Rhim et al. [28]. The transparency of the films was found to be reduced with the incorporation of nanoparticles in the nanocomposite's films due to the higher scattering of nanoparticles.

### 3.4. Scanning Electron Microscopy (SEM) of the Nanocomposite Film

Scanning electron microscopy (SEM) is a surface imaging method in which the incident electron beam scans across the sample surface and interacts with the sample to generate backscattered and secondary electrons that are used to create an image of the sample [39]. In order to compare the difference between the composite film and the composite with PVA and ZnO nanocomposite film, the specimens were characterized by the SEM analysis, and the corresponding SEM images were obtained (Figure 5a–c).

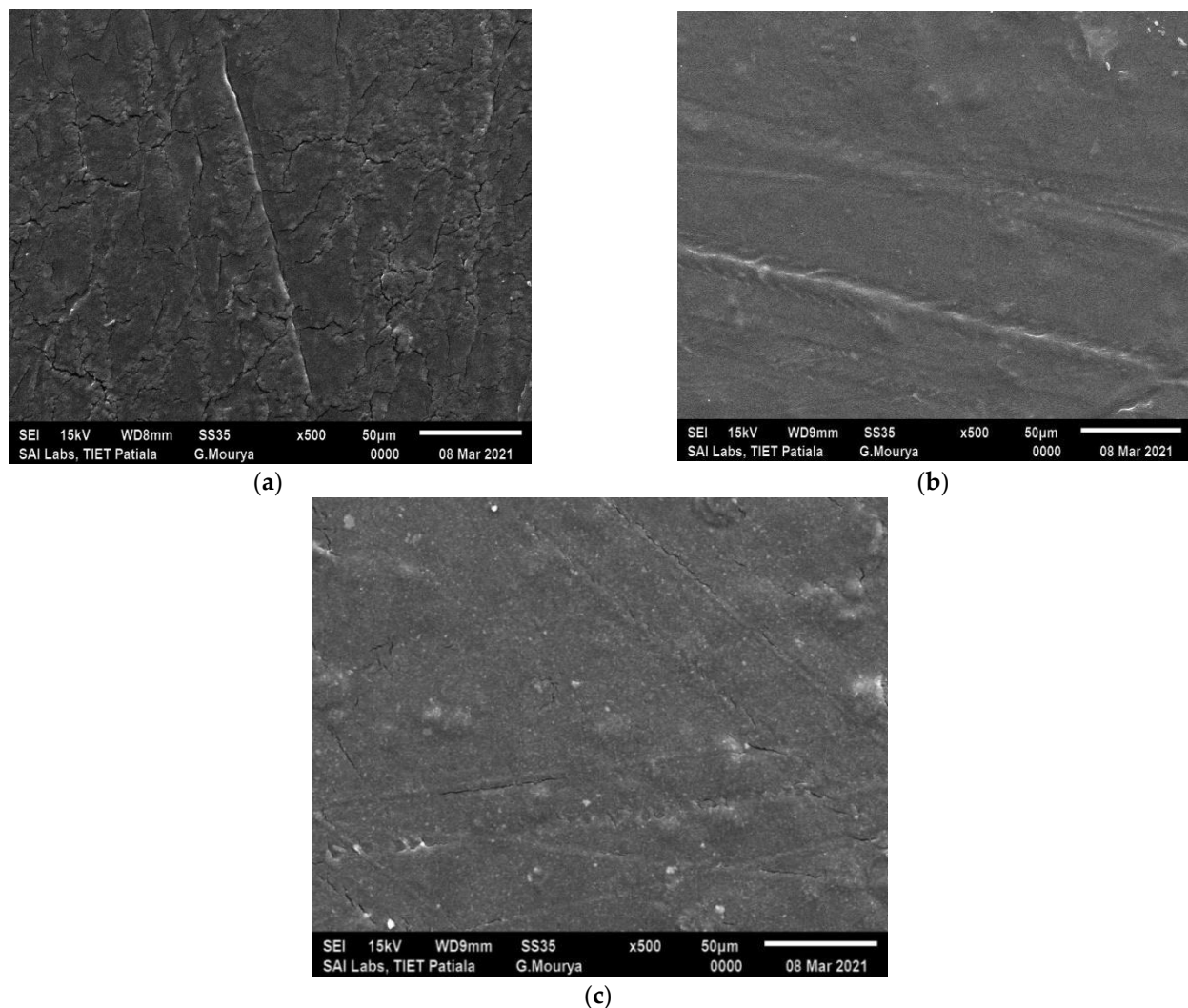


**Figure 5.** (a–c) Scanning electron microscopy of different types of films. (a) Composite film, (b) composite film with PVA, and (c) ZnO nanocomposite film.

In the SEM image of the ZnO nanocomposite film (Figure 5c), some of the nanoparticle aggregates were dispersed randomly in the polymer matrix. This might have been due to their high surface property. The ZnO nanocomposite film surface had roughness with

some small particle (white spot) aggregates. This indicates the segregation of ZnO in the polymeric matrixes, as potentially confirmed by the interaction and complexation between them. Good adhesion between the surface of the ZnO nanoparticles and the polymers was also shown in the film [31,40]. The representative SEM images of the composite (Figure 5a) and the composite with PVA (Figure 5b) film showed a good compact structure, with a smooth and flat appearance. The homogeneous matrix of films was a good indicator of their structural integrity, and consequently good mechanical properties could be expected by Mali et al. [41], Jayakumar et al. [42], and Atta et al. [31].

### 3.5. Biodegradation of Film

Biodegradation involves enzymatic and chemical degradation by living organisms. The biodegradation of the composite film was quicker compared to that of the composite with PVA and the composite with PVA and ZnO film, as shown in Figure 6. At the end of 50 days, there was a degradation of 96.22% in the composite film which was comparatively much faster than that of the composite with PVA and the composite with PVA and ZnO film, which were 92.33 and 89.25 per cent, respectively. When the nanoparticles were embedded in the films, the degradation was due to the decrease in both weight loss and water uptake. There were significant differences ( $p < 0.05$ ) between all the samples and there were also significant differences ( $p < 0.05$ ) between the days of all samples. Abbasi [43] also similarly observed that the addition of nanoparticles to the film led to slow degradation, and Azahari et al. [44] observed that the addition of PVA slowed down the rate of film degradation.

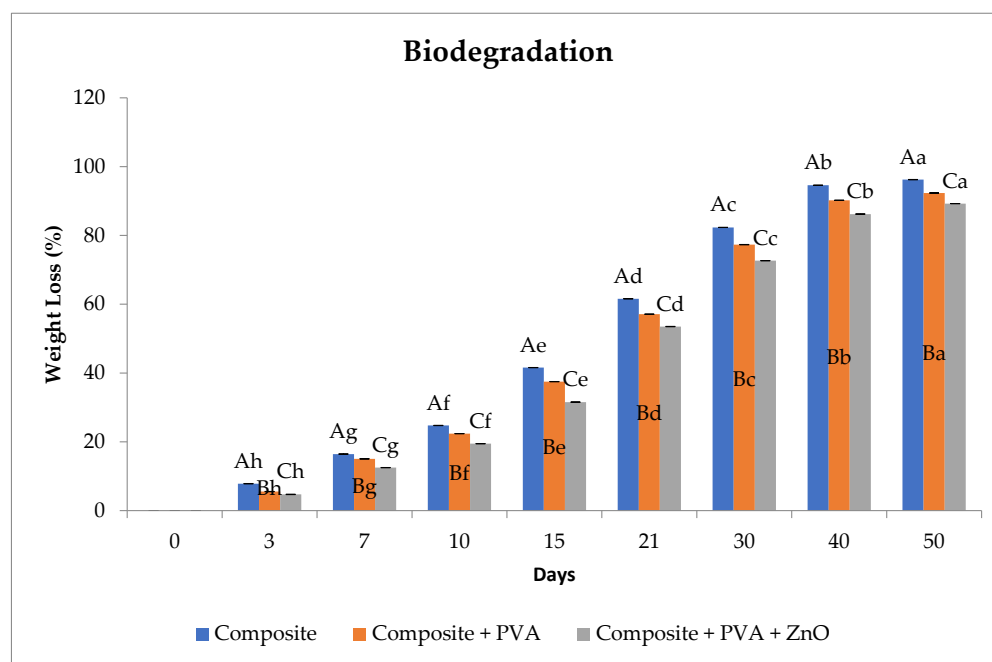


**Figure 6.** Biodegradation of different types of films. Figure representing the values (Mean  $\pm$  S.E.). A–C superscripts represent significant differences within samples on a particular day ( $p < 0.05$ ). a–h superscripts represent significant differences among different samples between days ( $p < 0.05$ ).

### 3.6. Antibacterial Activity of Nanoparticles Incorporated in Slurry and Film

From the research findings, it was found that the ZnO nanomaterial has antimicrobial properties for the inhibition of bacterial growth [45]. Based on the cell cytotoxicity results obtained by Singh [15], a 0.3% concentration of nanomaterials, such as ZnO, was selected for incorporation in the film for antibacterial enhancement. The level of inhibition was measured on the basis of the zone of inhibition test on solid media by both the well diffusion method (slurry) and the film adhesion method (film).

Below the 0.3% concentration of nanoparticles, ZnO did not exhibit antibacterial activity. However, at a 0.3% concentration of nanoparticles, results showed a 16 mm

inhibition zone by the well diffusion method against Gram-negative *E. coli* and a 17 mm inhibition zone against Gram-positive *B. cereus*. The film adhesion method with 0.3% ZnO nanoparticles showed an 18 mm inhibition zone against Gram-negative *E. coli* and a 20 mm inhibition zone against Gram-positive *B. cereus* (Figure 7B,D). Similarly, the control slurry (composite slurry/composite with PVA slurry) and the control film (composite film/composite with PVA film) did not manifest any antibacterial activity against *E. coli* and *B. cereus* (Figure 7A,C).

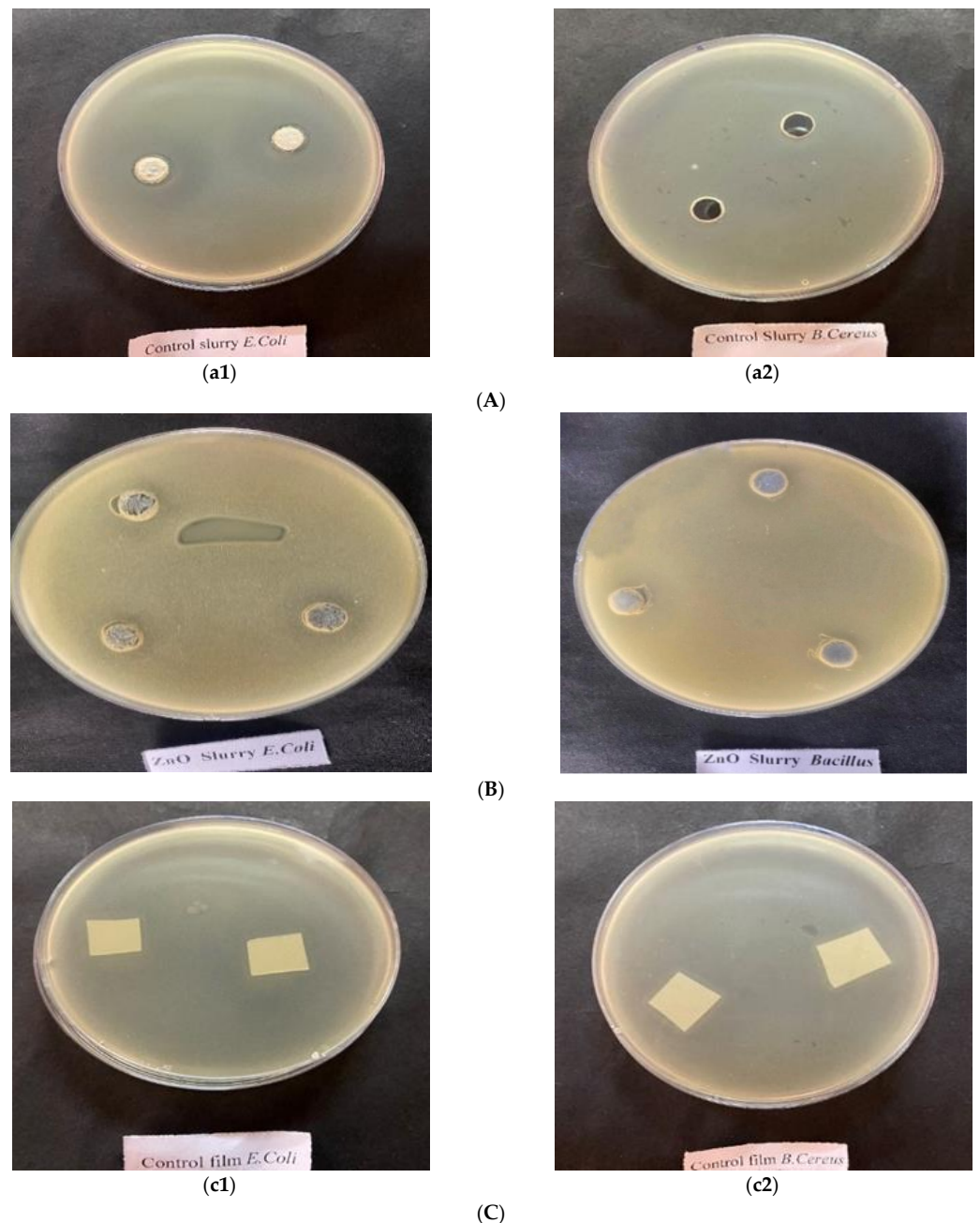
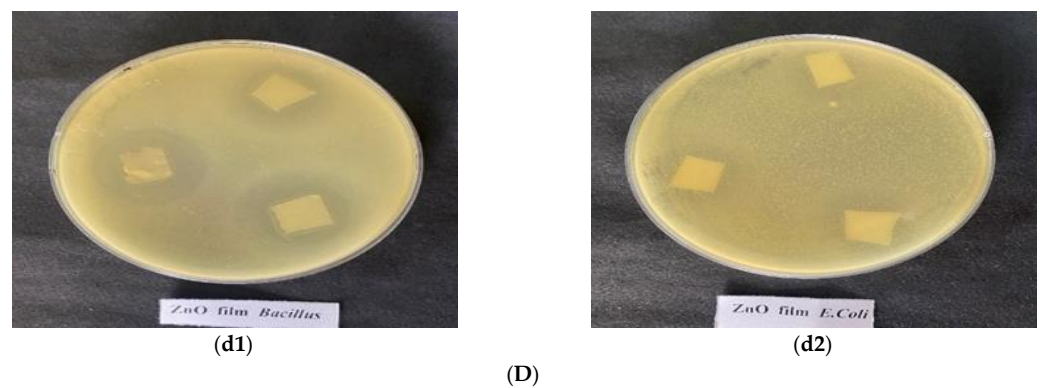


Figure 7. Cont.



**Figure 7.** (A) Control slurry: (a1) composite slurry; (a2) composite with PVA (antibacterial activity against *E. coli* and *B. cereus*) (B) ZnO nanocomposite Slurry (antibacterial activity against *E. coli* and *B. cereus*) (C) Control film: (c1) composite film; (c2) composite with PVA film (antibacterial activity against *E. coli* and *B. cereus*) (D): ZnO film: (d1) *Bacillus cereus*; (d2) *E. coli*. (antibacterial activity against tested organisms).

#### 4. Conclusions

The study concluded that the addition of PVA and ZnO particles in composite slurry improved various film properties, such as film thickness, WVP, film solubility, colour, and mechanical and antimicrobial properties, and that the values obtained differed significantly ( $p < 0.05$ ) between the treated and the control samples. The study also showed that the nanocomposite film prepared using a combination of corn starch (maize), whey protein concentrate and whey protein isolate, carrageenan, and PVA with added ZnO nanoparticles illustrated excellent mechanical, barrier, and antimicrobial properties, and could be an alternative to synthetic packaging materials. The developed package film has the potential to be used in the dairy industry, as well as in a variety of products for enhancing the shelf-life.

**Author Contributions:** Formal analysis, review, and writing: G.S.; conceptualization, methodology, original draft writing, and supervision: S.S.; investigation and editing: R.C.; review and editing: N.G.; software and data curation: G.T.; editing and resources: S.K.M.; resources: M.K.C. All authors have read and agreed to the published version of the manuscript.

**Funding:** This research received no external funding.

**Institutional Review Board Statement:** Not applicable.

**Informed Consent Statement:** Not applicable.

**Data Availability Statement:** All the relevant data are depicted in the form of figures and tables.

**Acknowledgments:** The authors gratefully acknowledge the research support provided by the College of Dairy Science and Technology, as well as the Research and the faculty of Guru Angad Dev Veterinary & Animal Sciences University (GADVASU).

**Conflicts of Interest:** The authors declare no conflict of interest.

#### References

1. Sorrentino, A.; Gorrasi, G.; Vittoria, V. Potential perspectives of bio-nanocomposites for food packaging applications. *Trends Food Sci. Technol.* **2007**, *18*, 84–95. [[CrossRef](#)]
2. De Azeredo, H.M. Nanocomposites for food packaging applications. *Food Res. Int.* **2009**, *42*, 1240–1253. [[CrossRef](#)]
3. Sothornvit, R.; Krochta, D.J. Plasticizer effect on oxygen permeability of  $\beta$ -lactoglobulin films. *J. Agric. Food Chem.* **2000**, *48*, 6298–6302. [[CrossRef](#)] [[PubMed](#)]
4. Sothornvit, R.; Krochta, J.M. Plasticizers in edible films and coatings. In *Innovations in Food Packaging*; Academic Press: Cambridge, MA, USA, 2005; pp. 403–433.
5. Han, Y.J.; Kim, S.S. Physical Properties of Mixed  $\kappa/\lambda$ - and  $\kappa/\iota$ -carrageenan Films. *Korean J. Food Sci. Technol.* **2008**, *40*, 42–46.

6. Jiménez, A.; Fabra, M.J.; Talens, P.; Chiralt, A. Effect of recrystallization on tensile, optical and water vapour barrier properties of corn starch films containing fatty acids. *Food Hydrocoll.* **2012**, *26*, 302–310. [[CrossRef](#)]
7. Kanatt, S.R.; Rao, M.S.; Chawla, S.P.; Sharma, A. Active chitosan–Poly Vinyl Alcohol films with natural extracts. *Food Hydrocoll.* **2012**, *29*, 290–297. [[CrossRef](#)]
8. DeMerlis, C.C.; Schoneker, D.R. Review of the oral toxicity of Poly Vinyl Alcohol (PVA). *Food Chem. Toxicol.* **2003**, *41*, 319–326. [[CrossRef](#)]
9. Karbowski, T.; Hervet, H.; Léger, L.; Champion, D.; Debeaufort, F.; Voilley, A. Effect of plasticizers (water and glycerol) on the diffusion of a small molecule in iota-carrageenan biopolymer films for edible coating application. *Biomacromolecules* **2006**, *7*, 2011–2019. [[CrossRef](#)]
10. Sogvar, O.B.; Saba, M.K.; Emamifar, A.; Hallaj, R. Influence of nano-ZnO on microbial growth, bioactive content and postharvest quality of strawberries during storage. *Innov. Food Sci. Emerg. Technol.* **2016**, *35*, 168–176. [[CrossRef](#)]
11. Vasile, C.; Râpă, M.; Ștefan, M.; Stan, M.; Macavei, S.; Darie-Niță, R.N.; Barbu-Tudoran, L.; Vodnar, D.C.; Popa, E.E.; Ștefan, R.; et al. New PLA/ZnO: Cu/Ag bionanocomposites for food packaging. *Express Polym. Lett.* **2017**, *11*, 531–544. [[CrossRef](#)]
12. Colon, G.; Ward, B.C.; Webster, T.J. Increased osteoblast and decreased Staphylococcus epidermidis functions on nanophase ZnO and TiO<sub>2</sub>. *J. Biomed. Mater. Res. A* **2006**, *78*, 595–604. [[CrossRef](#)]
13. Li, W.; Li, L.; Zhang, H.; Yuan, M.; Qin, Y. Evaluation of PLA nanocomposite films on physicochemical and microbiological properties of refrigerated cottage cheese. *J. Food Process. Preser.* **2018**, *42*, 13362. [[CrossRef](#)]
14. Singh, G.; Sivakumar, S.; Chawla, R.; Viji, P.C. Development and Characterization of Environment Friendly Starch and Protein Based Packaging Materials for Food Applications. *Int. J. Agric. Env. Biotechnol.* **2022**, *15*, 637. [[CrossRef](#)]
15. Singh, G. Process Optimization for the Development and Characterization of Nanobiocomposite Film Using Nanoparticles. Master's Thesis, Guru Angad Dev Veterinary and Animal Sciences University, Punjab, India, 2019.
16. Sivakumar, S.; Chawla, R.; Singh, N.; Singh, G. Effect of ultrasonication on properties of whey protein based nanobiocomposite film. In Proceedings of the National Conference on Emerging and Sustainable Technologies in Food Processing (ESTFP-2018), Longowal, India, 15–16 March 2018.
17. Sivakumar, S.; Chawla, R.; Singh, N.; Singh, G. From Synthetics to Natural, Growing Era of Edible Films (Starch vs. Protein). In Proceedings of the Third National Conference on Contemporary Food Processing and Preservation Technologies, Solan, India, 12–13 April 2018.
18. Singh, T.P.; Chatli, M.K.; Sahoo, J. Development of chitosan based edible films: Process optimization using response surface methodology. *J. Food Sci. Technol.* **2015**, *52*, 2530–2543. [[CrossRef](#)]
19. ASTM International. *ASTM E96-Standard Test Methods for Water Vapor Transmission of Materials*; ASTM International: West Conshohocken, PA, USA, 2000.
20. Al-Sahlany, S.T. Production of biodegradable film from soy protein and essential oil of lemon peel and use it as cheese preservative. *Basrah J. Agric. Sci.* **2017**, *30*, 27–35. [[CrossRef](#)]
21. Shokryazdan, P.; Sieo, C.C.; Kalavathy, R.; Liang, J.B.; Alitheen, N.B.; Faseleh Jahromi, M.; Ho, Y.W. Probiotic potential of Lactobacillus strains with antimicrobial activity against some human pathogenic strains. *BioMed Res. Int.* **2014**, *2014*, 927268. [[CrossRef](#)]
22. Gurpreet, K.; Singh, S.K. Review of nanoemulsion formulation and characterization techniques. *Indian J. Pharm. Sci.* **2018**, *80*, 781–789. [[CrossRef](#)]
23. Zayyoun, N.; Bahmad, L.; Laânab, L.; Jaber, B. The effect of pH on the synthesis of stable Cu<sub>2</sub>O/CuO nanoparticles by sol–gel method in a glycolic medium. *Appl. Phys.* **2016**, *122*, 488. [[CrossRef](#)]
24. Qi, J.; Ye, Y.Y.; Wu, J.J.; Wang, H.T.; Li, F.T. Dispersion and stability of titanium dioxide nanoparticles in aqueous suspension: Effects of ultrasonication and concentration. *Water Sci. Technol.* **2013**, *67*, 147–151. [[CrossRef](#)] [[PubMed](#)]
25. Marsalek, R. Particle size and zeta potential of ZnO. *APCBEE Procedia* **2014**, *9*, 13–17. [[CrossRef](#)]
26. Nanocomposix. *Zeta Potential Analysis of Nanoparticles*; Nanocomposix: San Diego, CA, USA, 2012.
27. Gharoy Ahangar, E.; Abbaspour Fard, M.H.; Shahtahmassebi, N.; Khojastehpour, M.; Maddahi, P. Preparation and characterization of PVA/ZnO nanocomposite. *J. Food Process. Preser.* **2015**, *39*, 1442–1451. [[CrossRef](#)]
28. Rhim, J.W.; Hong, S.I.; Park, H.M.; Ng, P.K. Preparation and characterization of chitosan-based nanocomposite films with antimicrobial activity. *J. Agric. Food Chem.* **2006**, *54*, 5814–5822. [[CrossRef](#)]
29. Ngo TM, P.; Dang TM, Q.; Tran, T.X.; Rachtanapun, P. Effects of zinc oxide nanoparticles on the properties of pectin/alginate edible films. *Int. J. Polym. Sci.* **2018**, *2018*, 5645797.
30. Yang, M.; Shi, J.; Xia, Y. Effect of SiO<sub>2</sub>, PVA and glycerol concentrations on chemical and mechanical properties of alginate-based films. *Int. J. Biol. Macromol.* **2018**, *107*, 2686–2694. [[CrossRef](#)]
31. Atta, A.; Abdel Reheem, A.M.; Abdeltwab, E. Ion beam irradiation effects on surface morphology and optical properties of ZnO/PVA composites. *Surf. Rev. Lett.* **2020**, *27*, 1950214. [[CrossRef](#)]
32. Nafchi, A.M.; Mahmud, S.; Robal, M. Antimicrobial, rheological, and physicochemical properties of sago starch films filled with nanorod-rich zinc oxide. *J. Food Eng.* **2012**, *113*, 511–519. [[CrossRef](#)]
33. Saputri, A.E.; Praseptiangga, D.; Rochima, E.; Panatarani, C.; Joni, I.M. Mechanical and solubility properties of bio-nanocomposite film of semi refined kappa carrageenan/ZnO nanoparticles. In *AIP Conference Proceedings*; AIP Publishing LLC: Melville, NY, USA, 2018; Volume 1927, p. 030040.



34. Akhavan, A.; Khoylou, F.; Ataeivarjovi, E. Preparation, and characterization of gamma irradiated Starch/PVA/ZnO nanocomposite films. *Radiat. Phys. Chem.* **2017**, *138*, 49–53. [[CrossRef](#)]
35. Ahmed, J.; Arfat, Y.A.; Castro-Aguirre, E.; Auras, R. Mechanical, structural and thermal properties of Ag–Cu and ZnO reinforced polylactide nanocomposite films. *Int. J. Biol. Macromol.* **2016**, *86*, 885–892. [[CrossRef](#)]
36. Wu, S.; Chen, X.; Yi, M.; Ge, J.; Yin, G.; Li, X.; He, M. Improving thermal, mechanical, and barrier properties of feather keratin/Poly Vinyl Alcohol/tris (hydroxymethyl) aminomethane nanocomposite films by incorporating sodium montmorillonite and TiO<sub>2</sub>. *Nanomaterials* **2019**, *9*, 298. [[CrossRef](#)]
37. Kumar, S.; Boro, J.C.; Ray, D.; Mukherjee, A.; Dutta, J. Bionanocomposite films of agar incorporated with ZnO nanoparticles as an active packaging material for shelf-life extension of green grape. *Heliyon* **2019**, *5*, e01867. [[CrossRef](#)]
38. Amjadi, S.; Emaminia, S.; Nazari, M.; Davudian, S.H.; Roufegarinejad, L.; Hamishehkar, H. Application of reinforced ZnO nanoparticle-incorporated gelatin bionanocomposite film with chitosan nanofiber for packaging of chicken fillet and cheese as food models. *Food Bioproc. Technol.* **2019**, *12*, 1205–1219. [[CrossRef](#)]
39. Ji, Z. Use of compositional and combinatorial nanomaterial libraries for biological studies. *Sci. Bull.* **2016**, *61*, 755–771. [[CrossRef](#)]
40. Paula, M.; Diego, I.; Dionisio, R.; Vinhas, G.; Alves, S. Gamma irradiation effects on polycaprolactone/zinc oxide nanocomposite films. *Polímeros* **2019**, *29*, e2019014-21. [[CrossRef](#)]
41. Mali, S.; Grossmann, M.V.E.; Garcia, A.; Martino, M.N.; Zaritzky, N.E. Microstructural characterization of yam starch films. *Carbohydr. Polym.* **2002**, *50*, 379–386. [[CrossRef](#)]
42. Jayakumar, A.; Heera, K.V.; Sumi, T.S.; Joseph, M.; Mathew, S.; Praveen, G.; Indu CNRadhakrishnan, E.K. Starch-PVA composite films with zinc-oxide nanoparticles and phytochemicals as intelligent pH sensing wraps for food packaging application. *Int. J. Biol. Macromol.* **2019**, *136*, 395–403. [[CrossRef](#)]
43. Abbasi, Z. Water resistance, weight loss and enzymatic degradation of blends starch/Poly Vinyl Alcohol containing SiO<sub>2</sub> nanoparticle. *J. Taiwan Inst. Chem. Eng.* **2012**, *43*, 264–268. [[CrossRef](#)]
44. Azahari, N.A.; Othman, N.; Ismail, H. Biodegradation studies of Poly Vinyl Alcohol/corn starch Corn starch (Maize)blend films in solid and solution media. *J. Phys. Sci.* **2011**, *22*, 15–31.
45. Zhang, L.; Jiang, Y.; Ding, Y.; Daskalakis, N.; Jeuken, L.; Povey, M.; York, D.W. Mechanistic investigation into antibacterial behaviour of suspensions of ZnO nanoparticles against *E. coli*. *J. Nanopart. Res.* **2010**, *12*, 1625–1636. [[CrossRef](#)]

**Disclaimer/Publisher’s Note:** The statements, opinions and data contained in all publications are solely those of the individual author(s) and contributor(s) and not of MDPI and/or the editor(s). MDPI and/or the editor(s) disclaim responsibility for any injury to people or property resulting from any ideas, methods, instructions or products referred to in the content.